

Supplementary Information for

**Tubular Dickkopf-3 promotes the development of renal atrophy  
and fibrosis**

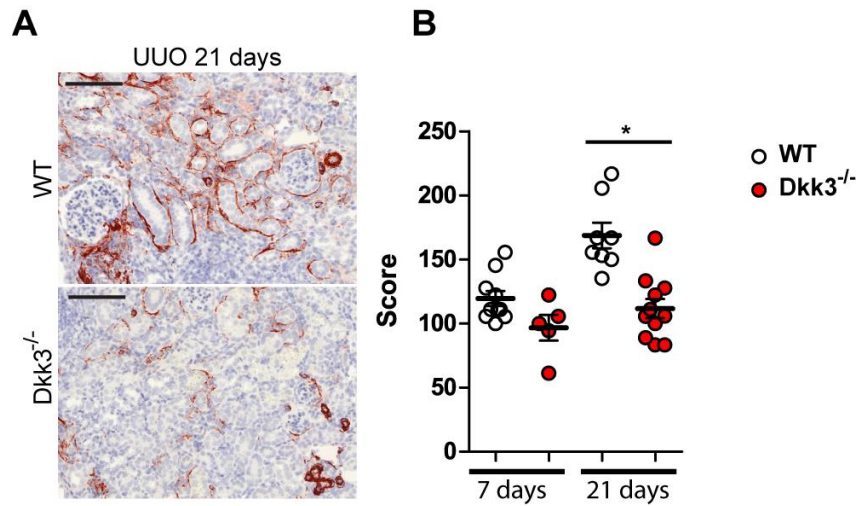
Giuseppina Federico<sup>1\*</sup> & Michael Meister<sup>2\*</sup>, Daniel Mathow<sup>1</sup>, Gunnar H. Heine<sup>3</sup>, Gerhard Moldenhauer<sup>2</sup>, Zoran V. Popovic<sup>1</sup>, Viola Nordström<sup>1</sup>, Annette Kopp-Schneider<sup>4</sup>, Thomas Hielscher<sup>4</sup>, Peter J. Nelson<sup>5</sup>, Franz Schaefer<sup>6</sup>, Stefan Porubsky<sup>1</sup>, Danilo Fliser<sup>3</sup>, Bernd Arnold<sup>2#</sup>, Hermann-Josef Gröne<sup>1#</sup>

**\*These authors contributed equally to the study**

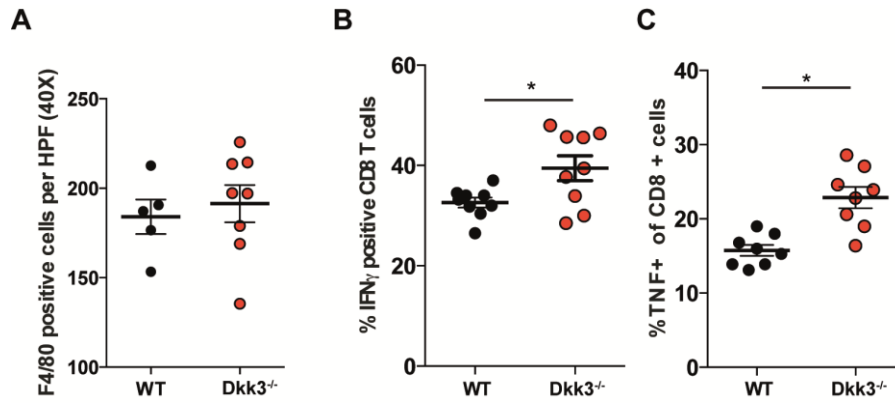
**#These authors share senior authorship**

**Correspondence to:**

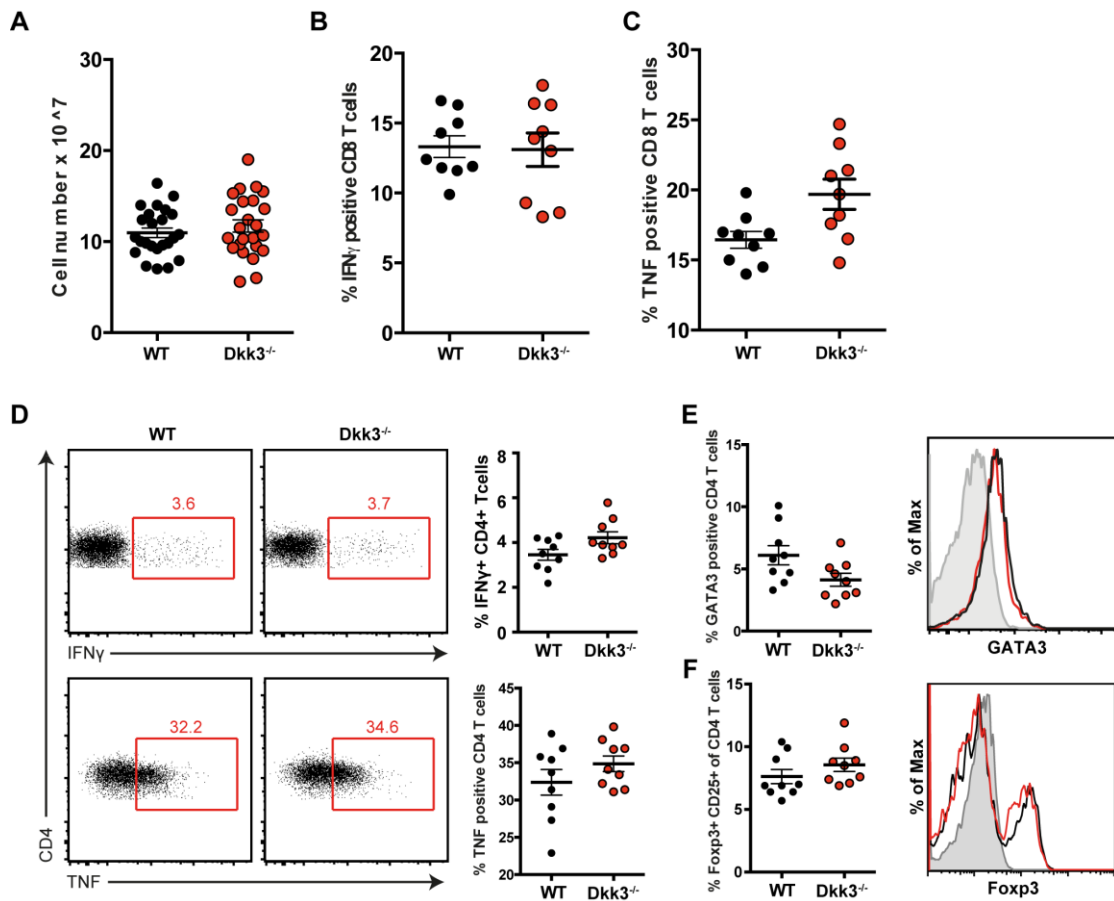
Hermann-Josef Gröne, Department of Cellular and Molecular Pathology, German Cancer Research Center, 69120 Heidelberg, Germany. Phone: 49.6221.42.4351; Fax: 49.6221.42.4363; E-mail: h.-j.groene@dkfz.de



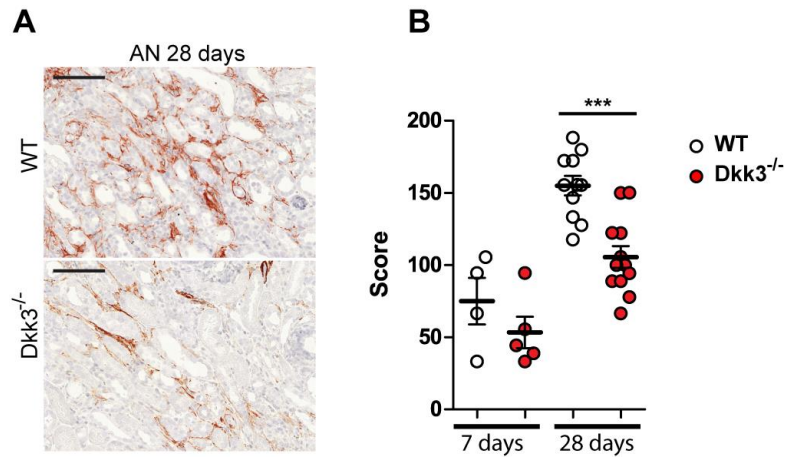
**Supplementary Figure 1. *Dkk3* promotes myofibroblast accumulation in the kidney upon unilateral ureteral obstruction (UUO).** (A) Representative images of alpha smooth muscle actin ( $\alpha$ -SMA)-stained kidney sections of *wildtype* (n=8) and *Dkk3*<sup>-/-</sup> (n=11) mice 21 days after UUO (Scale bar: 100 $\mu$ m). (B) Semi-quantitative analysis of renal interstitial fibrosis in  $\alpha$ SMA-stained kidney sections of *wildtype* (n=10/8) and *Dkk3*<sup>-/-</sup> (n=5/11) mice 7 and 21 days after UUO. All data are shown as mean  $\pm$  SEM. Statistical analysis performed using Mann-Whitney test. \*p-value<0.05.



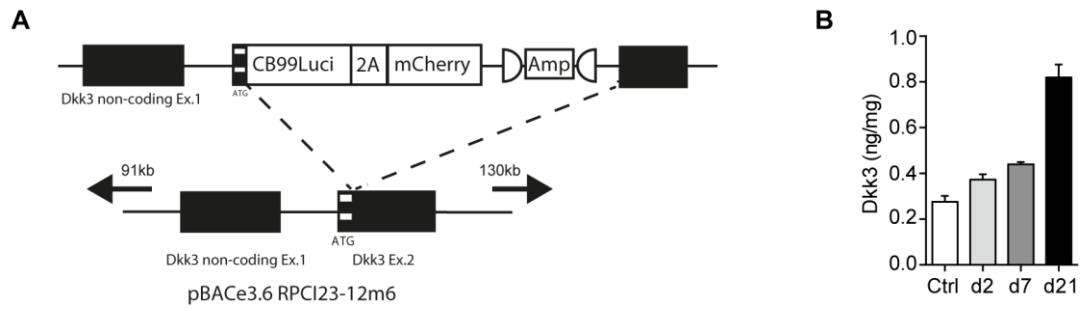
**Supplementary Figure 2. Dkk3 modulates CD8<sup>+</sup> T cell polarization but not macrophage abundance in obstructed kidneys.** (A) Quantification of F4/80<sup>+</sup> cells per high power field (40X) in kidney sections of *wildtype* (n=5) and *Dkk3*<sup>-/-</sup> (n=8) 21 days after unilateral ureteral obstruction (UUO). (B, C) Flow cytometric analysis of T cells isolated from *wildtype* and *Dkk3*<sup>-/-</sup> mice 21 days after UUO. Percentage of IFN $\gamma$  (n=9, *wildtype*; n=9, *Dkk3*<sup>-/-</sup>) and TNF $\alpha$ -producing CD8<sup>+</sup> cells (n=8, *wildtype*; n = 8, *Dkk3*<sup>-/-</sup>). All data are shown as mean  $\pm$  SEM. Statistical analysis performed using either Mann-Whitney test (A) or an unpaired, 2-tailed t-test (B, C). \*p-value<0.05.



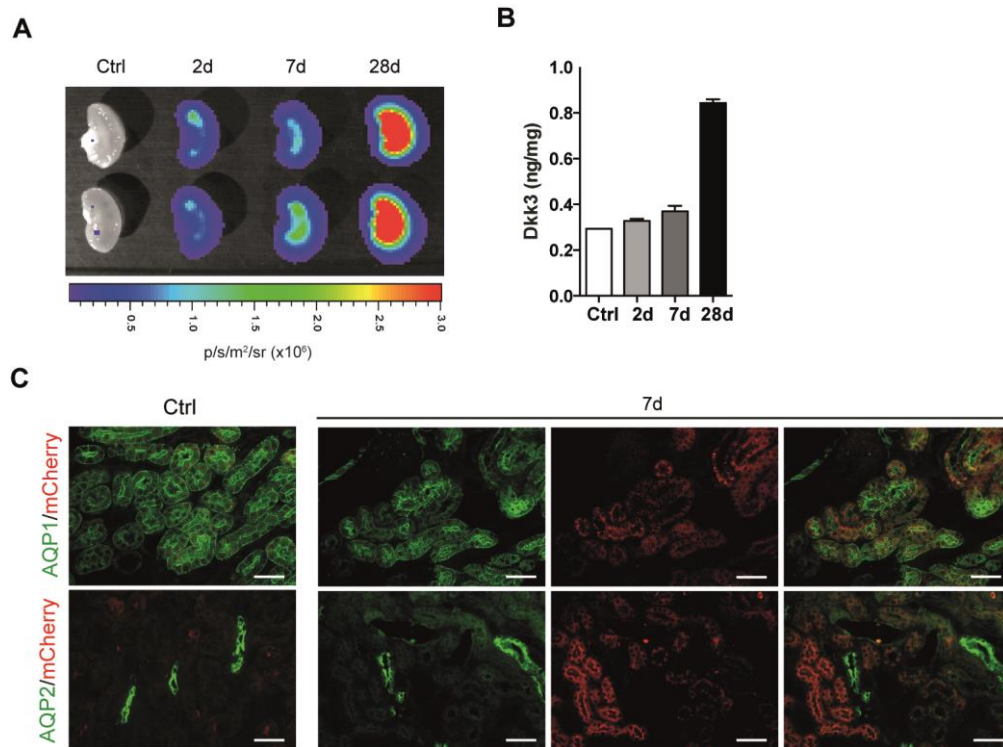
**Supplementary Figure 3. Dkk3 does not influence the T cell response in the spleen upon UOU.** (A) Splenocyte number of *wildtype* (n=24) and *Dkk3*<sup>-/-</sup> (n=24) mice 21 days after UOU. (B, C) Percentage of (B) IFN $\gamma$ <sup>+</sup> and (C) TNF<sup>+</sup> CD8<sup>+</sup> T cells in spleens of *wildtype* (n=9) and *Dkk3*<sup>-/-</sup> (n=9) mice 21 days after UOU analyzed by flow cytometry. (D) Flow cytometric analysis of IFN $\gamma$  and TNF producing CD4<sup>+</sup> T cells in spleens of *wildtype* (n=9) and *Dkk3*<sup>-/-</sup> (n=9) mice 21 days after UOU. Shown are representative dot plots (left panel) and cumulative data (right panel). (E) Percentages of GATA3<sup>+</sup> of CD4<sup>+</sup> cells (left panel) and respective GATA3 expression in CD4<sup>+</sup> T cells (right panel) in spleens of *wildtype* (n=9) and *Dkk3*<sup>-/-</sup> (n=9) mice, 21 days after UOU, analyzed by flow cytometry (F) Percentages of CD25<sup>+</sup>Foxp3<sup>+</sup> of CD4<sup>+</sup> cells (left panel) and respective Foxp3 expression in CD4<sup>+</sup> T cells (right panel) in spleens of *wildtype* (n=9) and *Dkk3*<sup>-/-</sup> (n=9) mice, 21 days after UOU, analyzed by flow cytometry. All data are shown as mean  $\pm$  SEM. Statistical analysis performed using an unpaired, 2-tailed t-test.



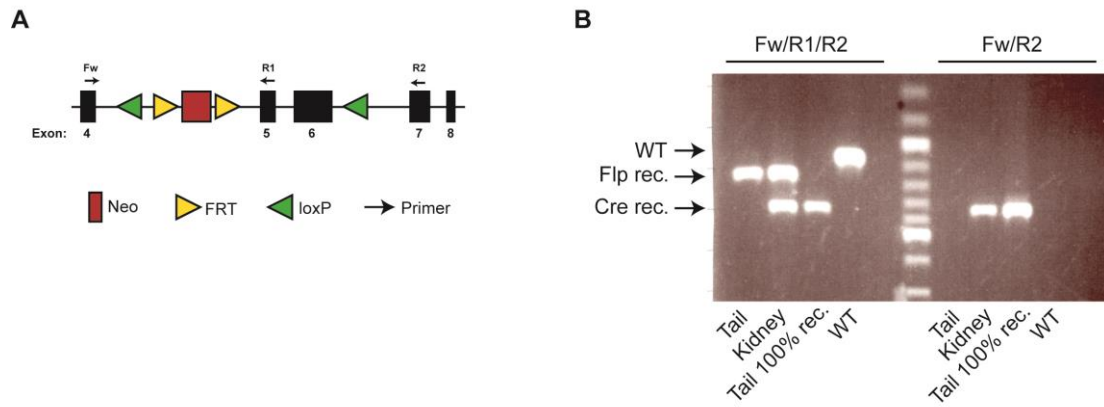
**Supplementary Figure 4. *Dkk3* promotes myofibroblast accumulation in the kidney during in adenine nephropathy.** (A) Representative images of alpha smooth muscle actin ( $\alpha$ -SMA)-stained kidney sections of *wildtype* (n=11) and *Dkk3*<sup>-/-</sup> (n=12) mice 28 days after adenine-rich diet administration (Scale bar: 100 $\mu$ m). (B) Semi-quantitative analysis of renal interstitial fibrosis in  $\alpha$ SMA-stained kidney sections of *wildtype* (n=4/11) and *Dkk3*<sup>-/-</sup> (n=5/12) mice 7 and 28 days after adenine-rich diet administration. All data are shown as mean  $\pm$  SEM. Statistical analysis performed using Mann-Whitney test. \*\*\*p-value<0.001.



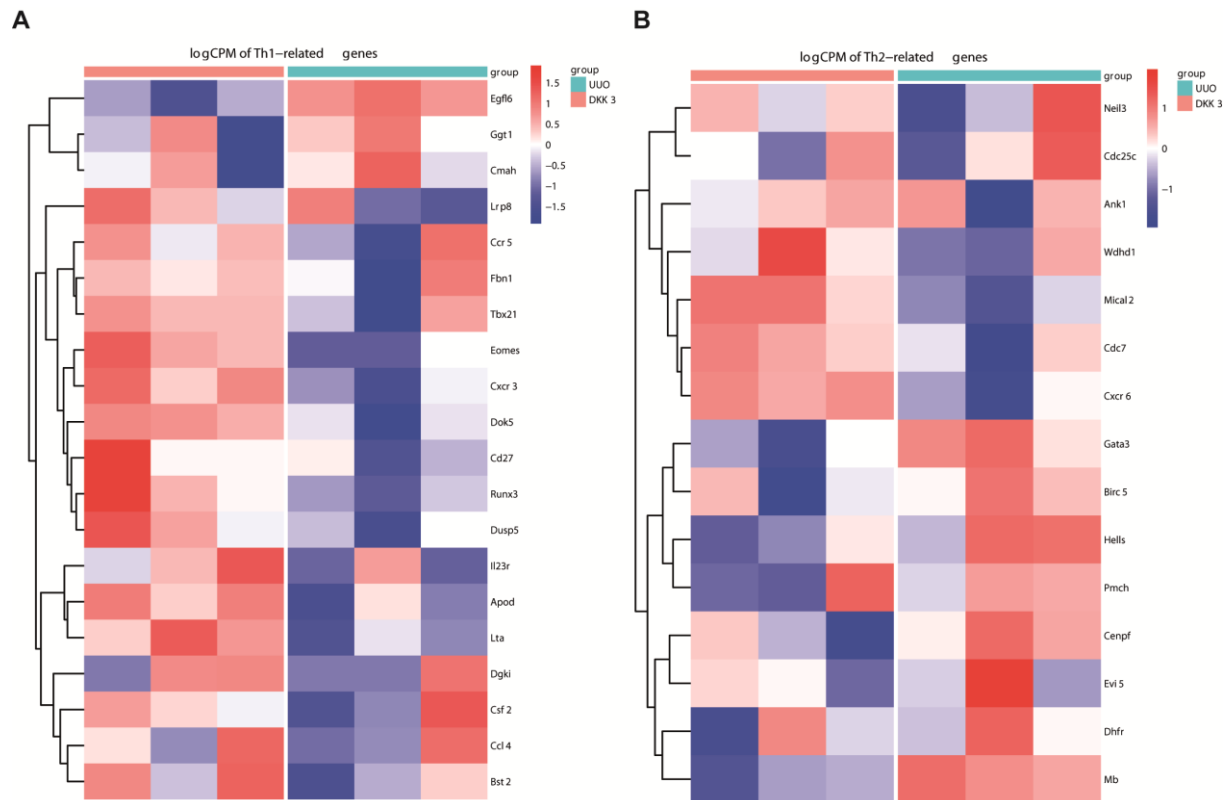
**Supplementary Figure 5. Dkk3 expression in kidney is induced upon unilateral ureteral obstruction (UUO).** (A) Schematic illustration of the *Dkk3-LCh* mouse DNA construct. (B) ELISA based Dkk3 protein detection in lysates of non-perfused kidneys before and 2, 7 and 21 days after UUO.



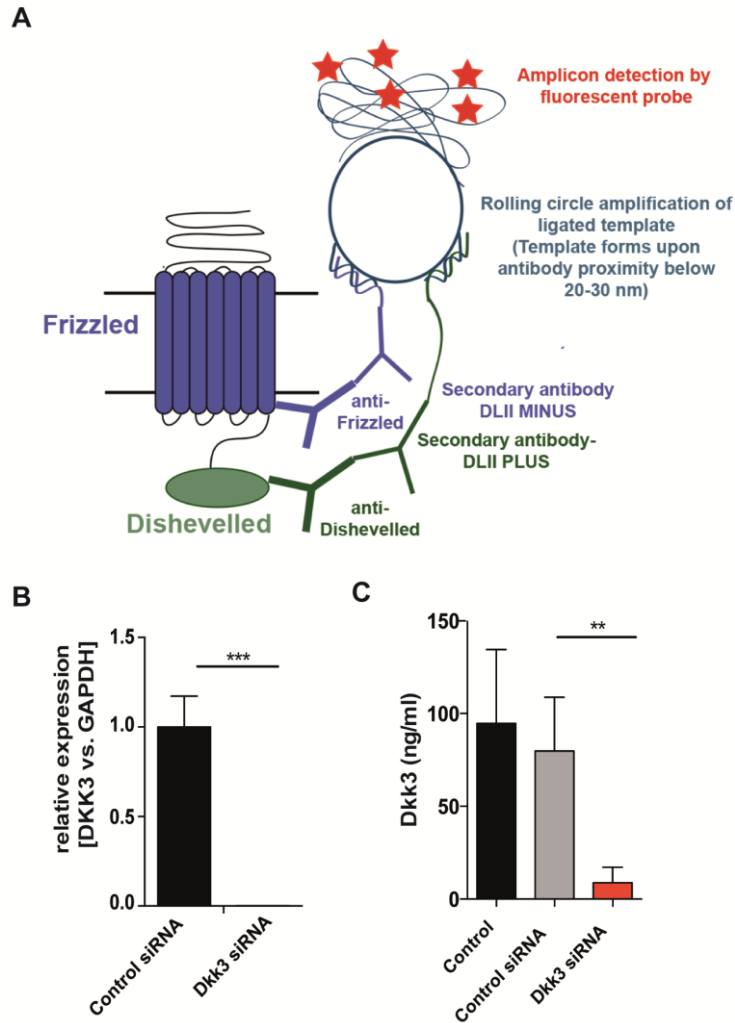
**Supplementary Figure 6. Tubular epithelial cells are the predominant source of renal, pro-fibrotic Dkk3 in adenine nephropathy.** (A) Representative ex vivo bioluminescence images (n=3) of kidneys of *Dkk3-LCh* mice 0, 2, 7, and 28 days after beginning of an adenine-rich diet. (B) ELISA measurements of Dkk3 protein in non-perfused adenine-induced kidney lysate at 2, 7, 28 days, and in non-perfused untouched tissue (Ctrl). (C) Representative immunofluorescence images of *Dkk3-LCh* mouse kidneys, before (Ctrl) and 7 days after unilateral ureteral obstruction (UUO), stained for mCherry (red) / aquaporin 1 (AQP1, green) (upper panel), or mCherry (red) / aquaporin 2 (AQP2, green) (lower panel) (n=4) (Scale bar=100 $\mu$ m).



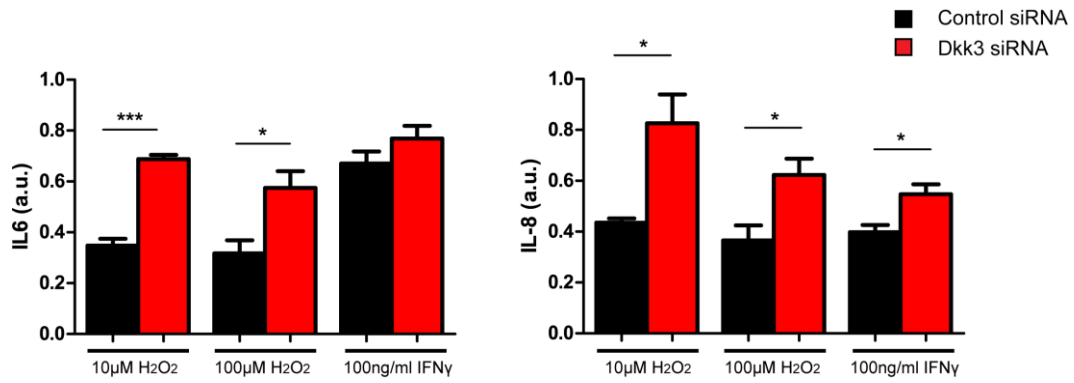
**Supplementary Figure 7. Characterization of the tubular specific DKK3 deficient mouse.** (A) Schematic illustration of the *Dkk3<sup>fl/fl</sup>* mouse DNA construct. (B) Gel electrophoresis showing *Dkk3<sup>fl/fl</sup>* x *Pax8<sup>+Cre</sup>* mouse genotyping.



**Supplementary Figure 8. RNA-seq analysis reveals a shift of T cell polarization in *Dkk3*<sup>-/-</sup> kidneys upon unilateral ureteral obstruction (UUO).** (A) Heatmap representing Th1-related gene in either *Dkk3*<sup>-/-</sup> or *wildtype* mice 7 days after UUO. (B) Heatmap representing Th2-related gene in either *Dkk3*<sup>-/-</sup> or *wildtype* mice 7 days after UUO. Read counts were transformed to log<sub>2</sub> counts-per-millions (cpm) and scaled for visualization.



**Supplementary Figure 9. SiRNA efficiently blocks DKK3 production in HK2 cells.** (A) Schematic illustration of the proximity ligation assay (PLA). The close proximity (20-30nm) between the two target epitopes (Frizzled and Dishevelled) leads to the ligation of the PLA probe oligonucleotides in order to form a template. Thus, a rolling circle amplification step is enabled. The consequent amplified sequences are recognized by fluorescently labeled probes, and the presence of proximity ligation events results in fluorescent spots. (B, C) Analysis of DKK3 siRNA efficiency measured on mRNA level by qRT-PCR (B) or on protein level by ELISA (C) in untreated (control, n=3), and transfected cells (control siRNA, n=3, and DKK3 siRNA, n=3). All data are shown as mean  $\pm$  SEM. Statistical analysis performed using an unpaired, 2-tailed t-test. \*\*p-value<0.01; \*\*\*p-value<0.001.



**Supplementary Figure 10. DKK3 regulates stress-induced cytokine production in tubular epithelial cells.** Measurements of interleukin-6 (IL-6) (A) and interleukin-8 (IL-8) (B) protein levels in the supernatant of HK2 cells treated either with control- or DKK3-siRNA and exposed to either H<sub>2</sub>O<sub>2</sub> (10μM or 100μM), or interferon-gamma (IFNγ) (100ng/ml) for 24 hours. Data are normalized to respective cytokine levels in the supernatant of control or DKK3-siRNA treated HK2 cells. All data are shown as mean ± SEM. Statistical analysis performed using Mann-Whitney test. \*p-value<0.05; \*\*\*p-value<0.001.

**Supplementary Table 1.** Pediatric CKD patients' cohort samples and related gender, age and main kidney disease diagnosis.

Samples		Gender		Age (Years)		Main Kidney Disease Diagnosis	Number
Number	Male	Female	Average	Range			
						Nephronophthise	37
72	44	28	13,57	6.7-19.4		Glomerulonephritis	35

**Supplementary Table 2.** Adult CKD patients' cohort samples and related gender, age and main kidney disease diagnosis.

Samples		Gender		Age (Years)		Main Kidney Disease Diagnosis	Number
Number	Male	Female	Average	Range			
						Transplanted Kidney	11
						Glomerulonephritis	11
						Focal Segmental Glomerulosclerosis	6
						Thrombotic Microangiopathy	2
34	21	13	58,03	22-79		Acute Kidney Damage	2
						Chronic Interstitial Nephritis	1
						Nephrosclerosis	1

**Supplementary Table 3.** Spearman's rank correlation coefficients and related p-values derived for DKK3 and either percentage or grade of fibrosis, DKK3 and either percentage or grade of tubular atrophy, DKK3 and either percentage or grade of IFTA (interstitial fibrosis/tubular atrophy).

DKK3 and...	Spearman rank correlation coefficient	p-value
Fibrosis %	0.71100	<0.0001
Fibrosis Grade	0.67983	<0.0001
Tubular Atrophy %	0.60571	0.0001
Tubular Atrophy Grade	0.55802	0.0006
IFTA %	0.67884	<0.0001
IFTA Grade	0.63786	<0.0001

**Supplementary Table 4.** Spearman's rank correlation coefficients and related p-values derived for Creatinine and either percentage or grade of fibrosis, Creatinine and either percentage or grade of tubular atrophy, Creatinine and either percentage or grade of IFTA (interstitial fibrosis/tubular atrophy).

Creatinine and...	Spearman rank correlation coefficient	p-value
Fibrosis %	0.52581	0.0014
Fibrosis Grade	0.50842	0.0021
Tubular Atrophy %	0.47916	0.0041
Tubular Atrophy Grade	0.44279	0.0087
IFTA %	0.52295	0.0015
IFTA Grade	0.49044	0.0032